

1 **PSMA-GCK01 - A Generator-Based $^{99m}\text{Tc}/^{188}\text{Re}$ -Theranostic Ligand for the**
2 **Prostate-Specific Membrane Antigen**

3 Running title: (Pre)clinical evaluation of PSMA-GCK01

4 Jens Cardinale^{1,2,*}, Frederik L. Giesel^{1,2,*}, Christina Wensky^{1,3}, Hendrik G. Rathke¹, Uwe Haberkorn^{1,3}, Clemens
5 Kratochwil¹

6 ¹Department of Nuclear Medicine, University Hospital Heidelberg, Heidelberg, Germany. ²Department of Nuclear
7 Medicine, Medical Faculty and University Hospital Duesseldorf, Heinrich-Heine-University Duesseldorf, Germany.

8 ³Clinical Cooperation Unit Nuclear Medicine, German Cancer Research Center (DKFZ), Heidelberg, Germany

9 * Contributed equally

10 Disclaimer: none

11 Corresponding / first author:

12 Jens Cardinale (PhD)

13 University hospital Duesseldorf (14.83), Moorenstrasse 5, 40225 Duesseldorf, Germany

14 Phone: +49(0)211 81 18874

15 Fax: +49(0)211 81 17041

16 Email: Jens.cardinale@med.uni-duesseldorf.de

17 Word Count: 4995

18 This work received financial support from Telix Pharmaceuticals Ltd.

19 Immediate Open Access: Creative Commons Attribution 4.0 International License (CC BY) allows users to share
20 and adapt with attribution, excluding materials credited to previous publications.

21 License: <https://creativecommons.org/licenses/by/4.0/>.

22 Details: <https://jnm.snmjournals.org/page/permissions>.

23



20 **ABSTRACT**

21 **Introduction:** Prostate-specific membrane antigen (PSMA)-theranostic has been introduced with Gallium-68 and
22 Lutetium-177, the currently most used radionuclides. However, Rhenium-188 is a well-known generator based
23 therapeutic nuclide completing a theranostic tandem with Technetium-99m and may offer an interesting alternative
24 to the current state of the art. In the present work, we aimed towards the development of a PSMA-targeted ^{99m}Tc -
25 ^{188}Re -theranostic tandem.

26 **Methods:** The ligand HYNIC-iPSMA was chosen as lead structure. Its HYNIC chelator has limitations for ^{188}Re -labeling
27 and was exchanged by MAS_3 to obtain PSMA-GCK01, as precursor for stable ^{99m}Tc - and ^{188}Re -labeling. ^{99m}Tc -PSMA-
28 GCK01 was used for the *in-vitro* evaluation of the novel ligand and comparison with ^{99m}Tc -EDDA/HYNIC-iPSMA. Planar
29 imaging using ^{99m}Tc -PSMA-GCK01 and organ biodistribution with ^{188}Re -PSMA-GCK01 were done using LNCaP-tumor
30 bearing mice, respectively. Finally, the theranostic tandem was applied for imaging and therapy in three prostate
31 cancer patients in compassionate care.

32 **Results:** An efficient radiolabeling of PSMA-GCK01 with both radionuclides was demonstrated. Cell-based assays with
33 ^{99m}Tc -PSMA-GCK01 vs ^{99m}Tc -EDDA/HYNIC-iPSMA revealed comparable uptake characteristics. Planar imaging and
34 organ distribution revealed a good tumor uptake of both, ^{99m}Tc - and ^{188}Re -PSMA-GCK01 at 1 h and 3 h p.i. with low
35 uptake in non-target organs. In patients, similar distribution patterns were observed for ^{99m}Tc -PSMA-GCK01 and
36 ^{188}Re -PSMA-GCK01 and also in comparison of Tc/Re-PSMA-GCK01 with ^{177}Lu -PSMA-617.

37 **Conclusion:** The novel ligand PSMA-GCK01 labels stable with ^{99m}Tc - and ^{188}Re - both are generator based
38 radionuclides – and, thus, provides access to on-demand labeling at reasonable costs. The preclinical evaluation of
39 the compounds revealed favorable characteristics of the PSMA-targeted theranostic tandem. This result was further
40 confirmed by a successful translation into first-in-human application.

41 **Key words:** PSMA, Rhenium-188, Technetium-99m, Theranostic, SPECT

42

43 INTRODUCTION

44 The development of novel theranostics has dominated the recent activities in the field of oncological nuclear
45 medicine. Most common theranostics are based on so-called matched pairs in which the diagnostic and therapeutic
46 radiopharmaceuticals are labeled with radionuclides from different elements – sometimes even different molecules
47 are used. The only precondition is that both (or all) radiopharmaceuticals within the matched pair show a very similar
48 biodistribution (1,2,3).

49 A combination of nuclides using the same precursor that perfectly fulfills this demand is Technetium-99m with
50 Rhenium-188 (and Rhenium-186) (4). Technetium-99m is still one of the most widely used radionuclides worldwide
51 and rhenium (with its isotopes Re-186 and Re-188) is the only element resembling its *in-vivo* chemistry nearly
52 perfectly. Moreover, both nuclides (Tc-99m and Re-188) are available from radionuclide generators disclosing
53 potential application in areas without strong nuclear infrastructure. Finally, Rhenium-188 might help to surpass
54 potential shortages in the supply of Lu-177, which may arise from lack of high-flux neutron facilities (5). This renders
55 technetium/rhenium-based theranostic radiopharmaceuticals an attractive combination, in particular for smaller
56 hospitals using “only” SPECT in their NM departments, as well as for application in developing countries (6). Another
57 more current aspect underscores the need for SPECT based PSMA imaging and, therefore, Technetium-99m ligands:
58 the patient selection for the recently approved ¹⁷⁷Lu-PSMA-617 (Pluvicto) affords confirmation of sufficient PSMA
59 uptake in a preliminary diagnostic scan. For these mandatory diagnostic scans, current PET infrastructure may
60 demonstrate to be the bottleneck - A challenge that might be met by suitable SPECT ligands including ligands
61 primarily developed for diagnostic purpose (e.g., ^{99m}Tc-MIP-1404 (7) and ^{99m}Tc-EDDA/HYNIC-iPSMA (8)).

62 The aim of this work was to develop a ^{99m}Tc-/¹⁸⁸Re-theranostic tandem targeting the prostate-specific
63 membrane antigen (PSMA). As lead structure the ligand HYNIC-iPSMA was chosen, which is already in advanced
64 clinical stage in its Technetium labeled form ^{99m}Tc-EDDA/HYNIC-iPSMA (8,9,10). Technetium-99m is coordinated via
65 the HYNIC-chelator in ^{99m}Tc-EDDA/HYNIC-iPSMA. However, it is rather unlikely that HYNIC is a suitable chelator for
66 Rhenium-188 (6). Thus, we replaced the chelator in HYNIC-iPSMA by the more suitable MAS3 – a classical N₃S-
67 chelator, which is suitable for ¹⁸⁸Re-coordination (Figure 1) (11,12). In the following, we will provide a summary on
68 our research results thus far including first-in-man application under compassionate use.

69 MATERIALS AND METHODS

70 General

71 The precursor synthesis was accomplished by well-known standard methods and is described in the
72 supplementary information (13,14). The SnCl₂ for Rhenium reduction was trace metal basis and acquired from Merck
73 (Taufkirchen, Germany). The remaining chemicals for tracer synthesis were all Ph. Eur. or *ad injectabilia* grade and
74 acquired from Merck (Taufkirchen, Germany) or BBraun (Melsungen, Germany) or. Waters Sep-Pak Light Alumina N
75 cartridges, Sep-Pak Light QMA cartridges and Sep-Pak Light tC18 cartridges were purchased from Macherey und
76 Nagel (Dueren, Germany). Dionex OnGuard II Ag cartridges were purchased from Thermo Fischer (Schwerte,
77 Germany).

78 Technetium-99m was obtained from a TekCis generator (Curium, Berlin, Germany) in form of ^{99m}Tc-NaTcO₄ in
79 0.9 % saline according to the manufacturer instructions. Rhenium-188 was obtained in form of ¹⁸⁸Re-NaReO₄ from a
80 ¹⁸⁸W/¹⁸⁸Re generator (OnkoBeta GmbH, Garching, Germany) by elution with 10 mL 0.9 % saline (BBraun, Melsungen,
81 Germany). ^{99m}Tc-EDDA/HYNIC-iPSMA was produced from commercial kits according to the instructions. The reagent-
82 kits were acquired from Telix Pharmaceuticals Ltd (Brussels, Belgium).

83

84 Chemistry and Radiochemistry

85 ^{99m}Tc-labeling of PSMA-GCK01. Phosphate buffer for the labeling was prepared from 890 mg Na₂PO₄·2 H₂O in 9.5
86 mL water for injection and 0.5 mL 2 M NaOH (pH = 11.5-12.0). For ^{99m}Tc-labeling, 500-800 μL pertechnetate solution
87 (1.5-2.5 GBq / mL in 0.9 % saline) were mixed with 200 μL phosphate buffer, 100 μL tris(2-carboxyethyl)phosphin
88 (TCEP; 28.9 mg / mL in phosphate buffer) 20 μL precursor solution (1 mg / mL). The resulting mixture (pH 8.0-8.5)
89 was heated at 98 °C for 10 minutes. The mixture was diluted with approx. 1 mL of 0.9 % saline and passed through a
90 C-18 cartridge (SepPak plus light tC18, preconditioned with 5 mL EtOH, followed by 10 mL water). The product was
91 eluted with 1 mL 70 % ethanol and diluted with 9 mL PBS (prepared from 9 mL 0.9 % saline and 1 mL phosphatebuffer
92 concentrate, BBraun *ad injectabilia*, both). Finally, the product was passed through a 0.22 μm sterile filter. Aliquots

93 of the reaction mixture were withdrawn directly after the reaction, after cartridge separation (before dilution with
94 PBS) and of the final product formulation and analyzed by RP-HPLC.

95 *¹⁸⁸Re-labeling of PSMA-GCK01.* ¹⁸⁸Re was eluted from the ¹⁸⁸W/¹⁸⁸Re-generator using 10 mL 0.9 % NaCl. The eluate
96 was postprocessed according to ref. (15). Briefly, potential tungsten breakthrough was retained on an SepPak
97 Alumina(N) cartridge. The eluate was dechlorinated using a Dionex OnGuard II Ag cartridge and the perrhenate was
98 concentrated using a SepPak QMA cartridge, preconditioned with 5 mL 1 m K₂CO₃, followed by 10 mL deionized
99 water. The perrhenate was eluted from the QMA-cartridge using 1 mL of 0.9 % NaCl (BBraun).

100 A typical ¹⁸⁸Re-labeling mixture consisted of 120 µL citrate solution (100 mg / mL), 80 µL GCK-01 precursor
101 solution (1 mg/mL in MeCN/H₂O 50:50 v/v), 40 µL 30 % ascorbic acid solution (in water), 800 µL perrhenate in 0.9 %
102 NaCl (postprocessed as described above, 6-12 GBq) and 48 µL SnCl₂ (50 mg/mL in 1 m HCl). The pH of the mixture
103 was usually 2.0-3.5. The mixture was heated at 96 °C for 60 min. After cooling to ambient temperature, the mixture
104 was neutralized to a pH of 7.5 using 0.5 M sodiumphosphate, heated for additional 5 min at 96 °C, diluted with 1 mL
105 0.9 % NaCl and passed through a SepPak plus light tC18 cartridge (preconditioned with 5 mL Ethanol and 10 mL
106 water). The cartridge was washed with 2-3 mL 0.9 % NaCl and the product eluted with 1 mL 70 % EtOH. The solution
107 containing the product was diluted 1:9 into PBS (prepared from 9 mL 0.9 % NaCl and 1 mL sodiumphosphate
108 concentrate; BBraun *ad injectabilia*, both) containing 2 % sodium ascorbate solution. The (radiochemical) yield was
109 determined by division of the isolated product activity by the starting activity. The radiochemical purity was
110 determined by radio HPLC for the isolated product (after cartridge separation and formulation).

111

112 **Preclinical evaluation**

113 *In vitro and toxicological evaluation of ^{99m}Tc-/¹⁸⁸Re-PSMA-GCK01.* The evaluation has been conducted by well-
114 known standard methods (16,17). Detailed information is provided in the supplementary information.

115 Cellular uptake experiments were conducted in analogy to a previously described procedure (16). A detailed
116 description is provided in the supplementary information.

117

118 *In vivo and organ distribution experiments.* All animal experiments were conducted in compliance with the current
119 laws of the Federal Republic of Germany (Animal license number: 35-9185.81/G-127/(18). For *in vivo* planar imaging
120 and organ distribution experiments, 8-week-old BALB/c *nu/nu* mice (male) were subcutaneously inoculated in the
121 left shoulder 6 million LNCaP cells in 50 % Matrigel (Corning) in Opti-MEM I medium. The studies were performed
122 when the tumor size reached approx. 1 cm³ (8-12 weeks after inoculation). Mean body weight was 23 ± 2 g on the
123 day of investigation.

124
125 *In vivo planar imaging.* For the in-vivo planar imaging, 100 µL of a formulation containing 5-10 MBq ^{99m}Tc-labelled
126 compound in PBS (approx. 0.1 µg precursor, 1 nM, 5-10 MBq/nM) was injected into the tail vein of a LNCaP tumor
127 bearing mouse (n = 1). The animal was anesthetized with Isoflurane (Abbvie, Wiesbaden, Germany), placed on the
128 Gamma IMAGER – S/C (Paris, France) in prone position to perform planar imaging (using Gamma Acquisition und
129 GammaVision+ software). The scan was started directly after administration of the activity and the mouse was
130 scanned for 10 minutes. The scan was repeated after 30, 90, 180 minutes and 24 hours. An activity standard (approx.
131 1 MBq of the respective tracer) was prepared in a closed HPLC-sample flask and placed next to the animal during all
132 timepoints of the measurement.

133
134 *Ex vivo organ distribution with ¹⁸⁸Re-PSMA-GCK01.* For *ex-vivo* biodistribution, LNCaP tumor bearing mice were
135 injected with 100 µL of a PBS-formulation containing approx. 1 MBq of the respective ¹⁸⁸Re-PSMA-GCK01 (approx.
136 0.1 µg precursor, 1 µg precursor / mL), each. The animals were sacrificed by CO₂-asphyxiation at 1 h p.i. and 3 h p.i.,
137 respectively. Organs of interest were dissected, blotted dry, weighted and the radioactivity was determined on a
138 gamma counter (Packard Cobra II, GMI, Minnesota, USA) and calculated as % ID/g.

139
140 **Clinical imaging and therapy**

141 After written informed consent had been obtained, three patients with metastatic castration-resistant prostate
142 cancer received PSMA-RLT and the related companion diagnostic under compassionate care regulations. Prospective

143 clinical trial registration is not required for compassionate care that is performed under individual medical indication.
144 The ethical committee of the University Hospital Heidelberg approved the retrospective evaluation (permission S-
145 732/18). The patients were Gleason score 9 (N=2) or 10 (N=1), all were metastatic to lymph-nodes and bone but
146 without visceral lesions, all had previously received standard androgen-deprivation therapy,
147 abiraterone/prednisolone and docetaxel, N=2 had additionally received enzalutamide and N=1 apalutamide, N=2 had
148 additionally received cabazitaxel, all were BRCA1/2-wildtype and naïve to PARP-inhibitors, no one was a promising
149 candidate for $^{223}\text{RaCl}_2$ (low uptake in bone-scan or bulky lymph-nodes). One patient had previously received
150 Ipilimumab/Nivolumab and 2 cycles of $^{177}\text{Lu-PSMA-617}$, the other two patients were $^{177}\text{Lu-PSMA}$ -naïve.

151 To demonstrate target positive disease a diagnostic scan was performed approx. 1 week in advance of therapy
152 using 600 MBq $^{99\text{m}}\text{Tc-PSMA-GCK01}$ (molar activity: 75-125 MBq/nmol) and images were acquired 2-4 h p.i. with an
153 Low-Energy-High-Resolution collimator at 140 keV +/- 10% photopeak (E.Cam, Siemens, 18 cm/min). At the day-1 of
154 therapy 3.7 GBq $^{188}\text{Re-PSMA-GCK01}$ (molar activity 56-112 MBq/nmol) were administered, followed by serial planar
155 scans (20 min – 48 h as clinical available) centered at the 155 keV (+/-10%) photopeak, however with a High-Energy
156 collimator due to down-scatter of up to 2.12 MeV Bremsstrahlung (E.Cam, Siemens, 18 cm/min). After 1-2 d (approx.
157 2-3 physical half-lives of ^{188}Re), when septum-penetration of Bremsstrahlung became negligible, 3.7 GBq $^{177}\text{Lu-PSMA-}$
158 617 was injected and serial images were acquired with a Medium-Energy collimator; to avoid cross talk with the
159 primary 155 keV photons of Re-188 only the upper photopeak of Lu-177 at 210 keV (+/-10%) was used. Dual photo-
160 peak imaging within such a short time interval enables an intra-individual comparison of two therapeutic ligands,
161 while relevant treatment-related effects have not yet to be considered. The timeline of imaging time-points is
162 illustrated with Figure 2. However, under these circumstances no scatter-subtraction techniques could be applied to
163 obtain sufficient quantitative data.

164

165 **RESULTS**

166 **Chemistry and Radiochemistry**

167 *Precursor.* The identity of the precursor was confirmed by HPLC-MS $m/z = 977.386$ (calc. m/z ($[M+H]^+$) = 977.392)
168 and $m/z = 999.367$ (calc. m/z ($[M+Na]^+$) = 999.374). The purity was analyzed by HPLC and was larger than 95 %. The
169 only detectable impurity was the oxidized disulfide. Details are provided in supplementary Figures 1-3.

170 ^{99m}Tc-PSMA-GCK01. The radiosynthesis of ^{99m}Tc-PSMA-GCK01 reliably delivered the product in radiochemical
171 yields of 81 ± 3 % and purities above $97,8 \pm 0,7$ % after cartridge separation ($n = 8$). Molar activity was in the range of
172 75-125 MBq/nmol. Residual TCEP was removed quantitatively by cartridge separation. No signs of degradations were
173 observed over a period of 7h. Details are provided in supplementary Figures 4 and 5.

174 ¹⁸⁸Re-PSMA-GCK01. After Rhenium-188 postprocessing approx. 79 ± 6 % of the total activity was retrieved in 1 mL
175 of saline without any detectable tungsten-188 breakthrough ($n = 9$). Subsequent labeling yielded ¹⁸⁸Re-PSMA-GCK01
176 in radiochemical yields of 78 ± 3 % and with a radiochemical purity of more than 96 ± 3 % ($n = 6$). Molar activity was in
177 the range of 56-112 MBq/nmol. Only minor signs of degradation were observed after 3 h (approx. 3 % degradation
178 of RCP). Details are provided in supplementary Figure 6.

179

180 **Preclinical evaluation**

181 *In vitro evaluation.* The binding characteristics of PSMA-GCK01 and HYNIC-iPSMA were evaluated with the
182 respective ^{99m}Tc-labeled tracers; the results are summarized in Table 1. ^{99m}Tc-PSMA-GCK01 showed a plasma protein
183 binding of 98 %. The RCP of the free fraction showed no signs of degradation over 4h (by repetitive HPLC
184 measurements, see supplementary Figure 7).

185

186 *In vivo and organ distribution experiments.* The images acquired by *in vivo* planar imaging are shown in Figure 3. ROI
187 analysis and standardization on the internal standard provided a rough estimation of the observed uptake values of
188 ^{99m}Tc-PSMA-GCK01.

189 The results of the organ distribution of ^{188}Re -PSMA-GCK01 are depicted in Figure 4: The tumor uptake of the
190 ligand is approx. 5 % ID/g at 1 h p.i. rising to approx. 11 % ID/g at 3 h p.i.. Besides, the ligand showed an uptake of 70
191 % ID/g (1 h p.i.) and 91 % ID/g (3 h p.i.) in kidneys and 11 % ID/g (1 h p.i.) and approx. 4 % ID/g (3 h p.i.) in the spleen.
192 Moreover, renal excretion is reflected by urine “uptake” of 36 % ID/g (1 h p.i.) and 71 % ID/g (3h p.i.), respectively.
193 All further organs showed only minor tracer uptake. Detailed results are provided in the supplementary information.

194

195 *Toxicological investigation.* No test article-related mortality was observed. No difference in organ weights, or
196 macroscopic observations were made at terminal or recovery sacrifice.

197

198 **Clinical imaging and therapy**

199 In the three compassionate care patients, no acute adverse events were observed neither following injection
200 of $^{99\text{m}}\text{Tc}$ - nor ^{188}Re -PSMA-GCK01. Visually, the gross biodistribution of diagnostic $^{99\text{m}}\text{Tc}$ -PSMA-GCK01 was similar to
201 all other low-molecular-weight scintigraphic PSMA-ligands that have been developed previously (Figure 5a), with
202 combined renal and hepatointestinal clearance, non-target accumulation in salivary glands and low perfusion
203 dependent background in the remainder organs (8,9,18,19). Considering the limitations that the mono-energetic 140
204 keV pure gamma-emitting $^{99\text{m}}\text{Tc}$ -PSMA-GCK01 was imaged with a LEHR collimator but ^{188}Re -PSMA-GCK01 had to be
205 measured with a HE collimator to cope with the high level of scatter and bremsstrahlung (up to 2.12 MeV) in relation
206 to the only 15% co-emission probability of 155 keV photons, the tagged radionuclide had no obvious influence
207 regarding the biodistribution at 2-4 h p.i., respectively (Figure 5). Already 20 min p.i., the intensity of tumor targeting
208 exceeds the intra-vascular blood-pool and delineation of the bladder demonstrates moderate clearance kinetics. Late
209 images beyond 20 h p.i. demonstrate prolonged trapping in tumor lesions, additional hepatobiliary clearance into
210 the intestine and low residual uptake in other organs (Figure 5b), thus in some degree PSMA-GCK01 is following a
211 similar tumor-accumulation and excretion kinetics comparable with other Glu-Urea-based PSMA-ligands such as
212 MIP1095, PSMA-617 or PSMA-I&T (20,21,22).

213 Using the distinct photopeaks of Re-188 at 155 keV, 48 h later followed by Lu-177 imaged at 210 keV an intra-
214 individual comparison between ^{188}Re -PSMA-GCK01 and ^{177}Lu -PSMA617 within a 2 day interval is demonstrated in
215 Figure 6. While tumor-targeting is almost equal at 20-24 and 44-48 h p.i., the PSMA-GCK01 demonstrates initially a
216 higher liver-to-kidney uptake ratio which translates into better delineation of the intestine at 48 h p.i., which might
217 imply a slightly shift from renal to hepato-intestinal clearance for PSMA-GCK01 compared to PSMA-617.

218

219 **DISCUSSION**

220 The focus of our investigation was the development of a PSMA-ligand suitable for $^{99\text{m}}\text{Tc}$ - and ^{188}Re -labeling
221 based on the HYNIC-IPsMA lead structure. Since the suitability of HYNIC for ^{188}Re -labeling has been discussed
222 controversially (6), we replaced the HYNIC unit with a similar-in-size spacer, linked to mercaptoacetyltriserine
223 sequence as favorable chelator for radiolabeling with both Tc-99m and Re-188 (Figure 1). The precursor synthesis
224 was obtained in high purity of more than 95 %. The only detectable “impurity” was the oxidized disulfide derivate
225 (supplemental Figures 2 and 3), which is reduced to the desired precursor under the reductive labeling conditions.

226 The technetium labeling using TCEP as reducing agent delivered the product $^{99\text{m}}\text{Tc}$ -PSMA-GCK01 in high and
227 reproducible yields and purities. In general, the radiochemical purity would allow for direct application of the product
228 mixture containing the tracer. However, for clinical formulation we applied a cartridge separation of the tracer to get
229 rid of any residual TCEP, which was confirmed by HPLC analysis (supplemental Figure 5). The reducing agent may
230 impose a potential limitation: For broader application a kit should be developed using the more commonly applied
231 SnCl_2 as reducing agent.

232 In case of the ^{188}Re -labeling the desired ^{188}Re -PSMA-GCK01 was produced in yields of approx. 75% (isolated
233 after synthesis and purification) using relatively harsh conditions (low pH). The results are in good agreement with
234 previous reports on such reactions (23). However, under these conditions the product is formed in two stereoisomers
235 (supplemental Figure 6). We eventually converted the undesired isomer by terminal elevation of the pH to 7.0-7.5
236 and a short additional heating period. In case of the $^{99\text{m}}\text{Tc}$ -labeling the pH was sufficiently high to suppress formation

237 of the isomer. Thus, and since no isomer formation was observed in the plasma stability of ^{99m}Tc -PSMA-GCK01 (see
238 below), we do not consider the potential isomer formation as drawback.

239 For the preclinical evaluation we first compared our ligand ^{99m}Tc -PSMA-GCK01 with ^{99m}Tc -EDDA/HYNIC-iPSMA
240 in a cell based assay: Both compounds showed a comparable and specific uptake in LNCaP cells. Further displacement
241 experiment with ^{99m}Tc -PSMA-GCK01 also revealed a comparable K_i of 26 (vs. 38 for ^{99m}Tc -EDDA/HYNIC-iPSMA). The
242 ligand showed a relatively high plasma-protein binding of 98%. However, it is well-known for other PSMA ligands that
243 high plasma-protein binding does not necessarily impose a problem for clinical application, recently even dedicated
244 albumin-binding motifs have been suggested as an improvement when PSMA-ligands should be labeled with long
245 physical half-life nuclides (24,25). More importantly, the free fraction in plasma did not show any signs of
246 decomposition over a period of 4 hours. Unfortunately, we were not able to confirm this for the theranostic Rhenium
247 tandem ^{188}Re -PSMA-GCK01 due to insufficient count rate (only 15,5 % probability of 155 keV emissions) in the
248 respective HPLC samples. Hence, we decided to evaluate our ligands in a suitable animal model. In planar imaging
249 with ^{99m}Tc -PSMA-GCK01, the ligand presents promising tumor uptake and retention in the LNCaP xenotransplant and
250 moderate renal clearance according to semiquantitative ROI analysis. Quantitative data was obtained by further
251 organ distribution experiments with the Rhenium analogue ^{188}Re -PSMA-GCK01: As expected, the results reflected
252 the planar imaging quite well. Already at 1 h p.i. we observed intense tumor uptake reaching approx. 11 %ID/g at 3
253 h p.i.. In mice only renal clearance but minimal uptake in the liver was observed; However, it was already reported
254 for PSMA-617 that renal vs. hepato-intestinal clearance is not comparable between animal-studies and human
255 application (14,26). In sum, preclinically we achieved our goal to develop a promising PSMA-ligand for labeling with
256 both Technetium and Rhenium for theranostic application. A potential limitation of the current preclinical study is
257 the missing of a late timepoint (e.g., 24 or 48 h) in the organ distribution and a histopathological evaluation of
258 eventual radiation-induced kidney toxicity of ^{188}Re -PSMA-GCK01 in mice. However, a dedicated clinical dosimetry
259 study is already in preparation (including an initial extrapolation from ^{99m}Tc -PSMA-GCK01 to ^{188}Re -PSMA-GCK01),
260 which is probably more predictive than the mice-to-men extrapolation that are otherwise needed for non-radioactive
261 therapies. Another potential limitation is the missing of ^{99m}Tc -PSMA-GCK01 organ distribution data. We considered
262 this data facultative since analogy of ^{99m}Tc -/ ^{188}Re -radiopharmaceuticals is widely accepted (see e.g., Ref 4) and
263 consequently we preferred to reduced our demand for laboratory animals.

264 Toxicological investigation of PSMA-GCK01 according to current OECD guideline was ordered by a third-party
265 preclinical research organization and revealed no toxicological effect up to 2 mg/kg in mice. Based on this data we
266 conclude that GCK01 has a good safety profile and application of up to 2 µg/kg GCK01 in human will likely be well
267 tolerated.

268 During compassionate use the promising tumor-targeting and acceptable fast clearance kinetics was confirmed
269 in human beings. Dual photopeak-imaging enabled intra-individual comparison with the current standard-of-
270 reference compound ¹⁷⁷Lu-PSMA-617. Our preliminary investigation suggests that ¹⁸⁸Re-PSMA-GCK01 and ¹⁷⁷Lu-
271 PSMA-617 share the combined renal and hepato-intestinal clearance route and a relatively similar biodistribution
272 between 2 h p.i. and 20 hi. However, by using a double-isotope imaging protocol, a quantitatively reliable treatment
273 dosimetry could not be approximated, yet. Nevertheless, the novel ligands offer some promising benefits, which we
274 would summarize as follows:

- 275 • Availability of a completely generator based theranostic tandem to the currently available ligands will help
276 to facilitate PSMA-RLT, in particular in countries / regions with a less developed nuclear infrastructure. Moreover, it
277 may help to reduce cost of PSMA-RLT.
- 278 • ^{188/186}Re-PSMA-RLT might amend ¹⁷⁷Lu-PSMA-RLT in a “mixed nuclide therapy” with potential benefits in
279 offering additional beta-emission energy profile ($\beta_{\text{mean}}(\text{Re-188}) = 765 \text{ keV}$, $\beta_{\text{mean}}(\text{Re-186}) = 347 \text{ keV}$, $\beta_{\text{mean}}(\text{Re-Lu-177})$
280 $= 133 \text{ keV}$) improving therapy of bulk lesions (27,28).
- 281 • Shorter half-life and lower energy of gamma emission (Re-188: 16.9 h, 155 (15 %); Re-186: 3.7 d, 137 keV
282 (9%); Lu-177: 6.7 d, 113 keV (6%) & 208 (10 %)) may disclose therapy in an outpatient setting eventually helping to
283 circumvent the expected bottleneck in bed capacity of currently existing nuclear medicine departments after ¹⁷⁷Lu-
284 PSMA-617 (half-life 6.7 d) approval (29).

285 In summary, we consider the novel PSMA-ligands ^{99m}Tc-/¹⁸⁸Re-PSMA-GCK01 a versatile and promising
286 supplement in the currently available PSMA-ligand landscape. In particular, the broad availability of different
287 therapeutic nuclides may lead to interesting synergetic effects, which cannot be predicted by now. A phase I/II clinical

288 trial with the novel ligands including dosimetry study is currently in preparation. The additional potential which may
289 arise from the ligand ¹⁸⁶Re-GCK01 is still to be disclosed.

290

291 **CONCLUSION**

292 PSMA-GCK01 is characterized by robust labeling with both radionuclides of the theranostic ^{99m}Tc-PSMA-GCK01
293 / ¹⁸⁸Re-PSMA-GCK01 tandem, hence, they can be produced in high radiochemical yields using standard
294 methodologies, respectively. Preliminary experiences in patients with metastatic castration-resistant prostate cancer
295 were promising and thus further investigation of ^{99m}Tc/¹⁸⁸Re-PSMA-GCK01 in a prospective phase-1 trial was already
296 initiated.

297

298 **DISCLOSURE**

299 FLG, CK, UH and JC are holding a patent application on PSMA-GCK01. This project was supported by a research
300 grant from Telix Pharmaceuticals Ltd.. FLG is advisor at ABX Radiopharmaceuticals, SOFIE Biosciences, Telix pharma
301 and Alpha Fusion. The toxicological study at Agilix Biolabs was sponsored by Telix Pharmaceuticals Ltd..

302

303 **ACKNOWLEDGMENTS**

304 We thank the working group Haberkorn at Otto-Meyerhof-Zentrum Heidelberg – in particular Annette
305 Altmann, Marlene Tesch and Vanessa Kohl– for conducting the preclinical investigations. We thank Dr. Alesia
306 Ivashkevich and Dr. Michael Wheatcroft for their support and assistance of the toxicological study.

307

308 **KEY POINTS**

309 Question: Can we prepare a PSMA ligand suitable for ^{99m}Tc - and ^{188}Re -labeling based on HYNIC-iPSMA as lead
310 structure?

311 Pertinent Findings: An exchange of the chelator moiety to MAS_3 yielded PSMA-GCK01, a ligand suitable for
312 ^{99m}Tc - and ^{188}Re -labeling maintaining the good binding characteristics of HYNIC-iPSMA.

313 Implications for patient care: PSMA-GCK01 offers a suitable platform for the decentralized production of the
314 theranostic tandem for prostate cancer patients. In particular, it provides the basis for diagnosis of PCa in smaller
315 nuclear medical centers limited to SPECT and may help to circumvent potential bottlenecks in the Lutetium-177
316 supply chain.

317

318 **REFERENCES**

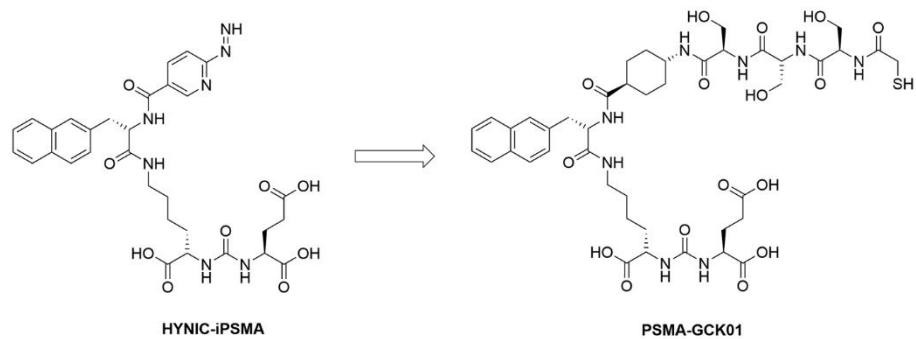
- 319 1. Herrmann K, Schwaiger M, Lewis JS, et al.. Radiotheranostics: a roadmap for future development. *Lancet*
320 *Oncol.* 2020;21:e146-156.
- 321 2. Barca C, Griessinger CM, Faust A, et al.. Expanding theranostic radiopharmaceuticals for tumor diagnosis
322 and therapy. *Pharmaceuticals MDPI.* 2022;15:13.
- 323 3. Solnes LB, Werner RA, Jones KM, et al.. Theranostics: leveraging molecular imaging and therapy to impact
324 patient management and secure the future of nuclear medicine. *J Nucl Med.* 2020;61:311-318.
- 325 4. Lepareur N, Lacoeyille F, Bouvry C, et al.. Rhenium-188 labeled radiopharmaceuticals: current applications
326 in oncology and promising perspectives. *Frontiers Med.* 2019;6:132.
- 327 5. Vogel VW, van der Marck SC, Versleijen MWJ. Challenges and future options for the production of
328 lutetium-177. *Eur J Nucl Med Mol Imaging.* 2021;48:2329-2335.
- 329 6. Blower PJ. Rhenium-188 radiochemistry: challenges and prospects. *International Journal of Nuclear*
330 *Medicine Research.* 2017:39-53.
- 331 7. Hillier SM, Maresca KP, Lu G, et al.. ^{99m}Tc-Labeled small-molecule inhibitors of prostate-specific membrane
332 antigen for molecular imaging of prostate cancer. *J Nucl Med.* 2013;54:1369-1376.
- 333 8. García-Pérez FO, Davanzo J, López-Buenrostro S, et al.. Head to head comparison performance of ^{99m}Tc-
334 EDDA/HYNIC-iPSMA SPECT/CT and ⁶⁸Ga-PSMA-11 PET/CT a prospective study in biochemical recurrence
335 prostate cancer patients. *Am J Nucl Med Mol Imaging.* 2018;8:332-340.
- 336 9. Ferro-Flores G, Luna-Gutiérrez M, Ocampo-García B, et al.. Clinical translation of a PSMA inhibitor for
337 ^{99m}Tc-based SPECT. *Nucl Med Biol.* 2017;48:36-44.
- 338 10. Santos-Cuevas C, Davanzo J, Ferro-Flores G, et al.. ^{99m}Tc-labeled PSMA inhibitor and radiation dosimetry in
339 healthy subjects and imaging of prostate cancer tumors in patients. *Nucl Med Biol.* 2017;52:1-6.
- 340 11. Chang F, Ruschkowski M, Qu T, Hnatowich DJ. Early results of the irrational design of new bifunctional
341 chelators. *Cancers* 1997;80(S12):2347-2352.
- 342 12. Chang F, Qu T, Ruschkowski M, Hnatowich DJ. NHS-MAS₃: a bifunctional chelator alternative to NHS-MAG₃.
343 *Appl Radiat Isot.* 1999;50:723-732.

- 344 13. Eder M, Schäfer M, Bauder-Wüst U, et al.. ⁶⁸Ga-complex lipophilicity and the targeting property of the
345 urea-based PSMA inhibitor for PET imaging. *Bioconjugate Chem.* 2012;23:688-697.
- 346 14. Benešová M, Schäfer M, Bauder-Wüst U, et al. Preclinical evaluation of a tailor made DOTA-conjugated
347 PSMA inhibitor with optimized linker moiety for imaging and endoradiotherapy of prostate cancer. *J Nucl*
348 *Med.* 2015;56:914-920.
- 349 15. Guhlke S, Beets AL, Oetjen K, Mirzadeh S, Biersack H-J, Knapp FF. Simple new method for effective
350 concentration of ¹⁸⁸Re solutions from alumina-based ¹⁸⁸W-¹⁸⁸Re generator. *J Nucl Med.* 2000;15:1271-
351 1278.
- 352 16. Lindner T, Loktev A, Altmann A, et al.. Development of quinoline-based theranostic ligands for the
353 targeting of fibroblast activation protein. *J Nucl Med.* 2018;59:1415-1422.
- 354 17. OECD (2008), Test No. 407: Repeated dose 28-day oral toxicity study in rodents, OECD guidelines for the
355 testing of chemicals, section 4, OECD publishing, Paris, <https://doi.org/10.1787/9789264070684-en>
356 (Accessed on 12.09.2022).
- 357 18. Vallabhajosula S, Nikolopoulou A, Babich JW, et al.. ^{99m}Tc-Labeled small-molecule inhibitors of prostate-
358 specific membrane antigen: pharmacokinetics and biodistribution studies in healthy subjects and patients
359 with metastatic prostate cancer. *J Nucl Med.* 2014;55:1791-1798.
- 360 19. Urbán S, Meyer C, Dahlbom M, et al.. Radiation dosimetry of ^{99m}Tc-PSMA-I&S: A single-center study. *J Nucl*
361 *Med.* 2021;62:1075-1081.
- 362 20. Zechmann CM, Afshar-Oromieh A, Amor T, et al.. Radiation dosimetry and first therapy results with a
363 ¹²⁴I/¹³¹I-labeled small molecule (MIP-1095) targeting PSMA for prostate cancer therapy. *Eur J Nucl Med*
364 *Mol Imaging.* 2014;41:1280-1292.
- 365 21. Kratochwil C, Giesel FL, Stefanova M, et al.. PSMA-targeted radionuclide therapy of metastatic castration-
366 resistant prostate cancer with ¹⁷⁷Lu-Labeled PSMA-617. *J Nucl Med.* 2016;57:1170-1176.
- 367 22. Weineisen M, Schottelius M, Simecek J, et al.. ⁶⁸Ga- and ¹⁷⁷Lu-Labeled PSMA I&T: optimization of a PSMA-
368 targeted theranostic concept and first proof-of-concept human studies. *J Nucl Med.* 2015;56:1169-1176.
- 369 23. Guhlke S, Schaffland A, Zamora PO, et al.. ¹⁸⁸Re- and ^{99m}Tc-MAG₃ as prosthetic groups for labeling amines
370 and peptides: approaches with pre- and postconjugate labeling. *Nucl Med Biol.* 1998;25:621-631.

- 371 24. Benešová M, Umbricht CA, Schibli R, Müller C. Albumin-binding PSMA ligands: optimization of the tissue
372 distribution profile. *Mol Pharmaceutics*. 2018;15:934-946.
- 373 25. Kelly JM, Amor-Coarasa, Ponalla S, et al.. Albumin-binding PSMA ligands: implications for expanding the
374 therapeutic window. *J Nucl Med*. 2019;60:656-663
- 375 26. Kabasakal L, AbuQbeidah M, Aygün A, et al.. Pre-therapeutic dosimetry of normal organs and tissues of
376 ¹⁷⁷Lu-PSMA-617 prostate-specific membrane antigen (PSMA) inhibitor in patients with castration-resistant
377 prostate cancer. *Eur J Nucl Med Mol Imaging*. 2015;42:1976-1983.
- 378 27. O'Donoghue JA, Bardiès, Wheldon TE. Relationships between tumor size and curability for uniformly
379 targeted therapy with beta-emitting radionuclides. *J Nucl Med*. 1995;36:1902-1909.
- 380 28. Strosberg J, Kunz PL, Hendifar A, et al.. Impact of liver tumour burden, alkaline phosphatase elevation, and
381 target lesion size on treatment outcomes with ¹⁷⁷Lu-Dotatate: an analysis of the NETTER-1 study. *Eur J Nucl*
382 *Med Mol Imaging*. 2020;47:2372-2382.
- 383 29. Zippel C, Giesel FL, Kratochwil C, et al.. PSMA-Radioligandentherapie könnte Nuklearmedizin vor
384 infrastrukturelle Herausforderungen stellen: Ergebnisse einer Basiskalkulation zur Kapazitätsplanung
385 nuklearmedizinischer Betten im deutschen Krankenhaussektor. *Nuklearmedizin*. 2021;60:216-223.

386

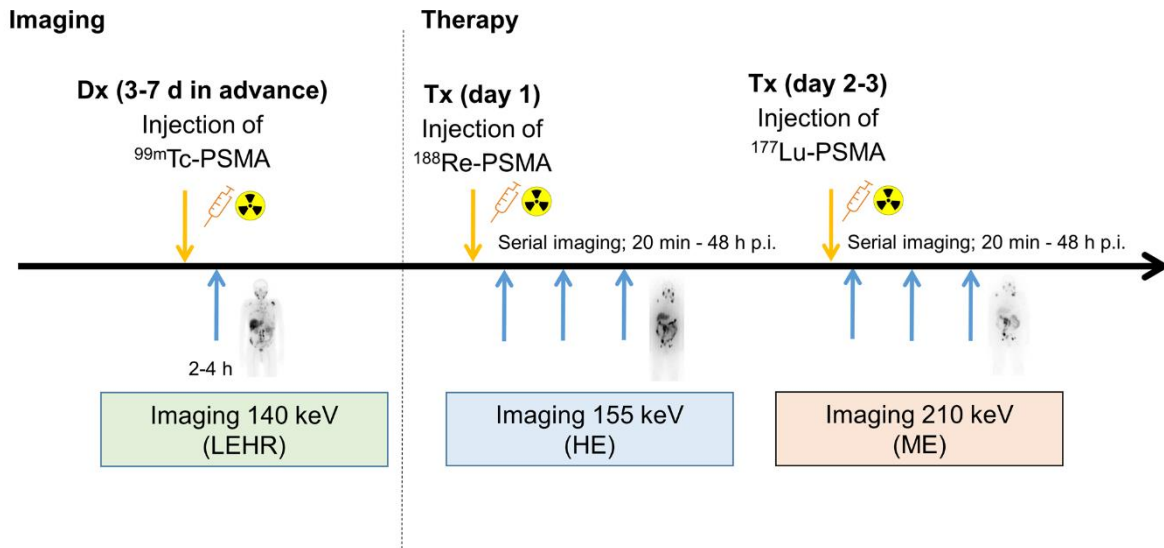
387



388

389 *Figure 1: Structures of HYNIC-iPSMA and PSMA-GCK01*

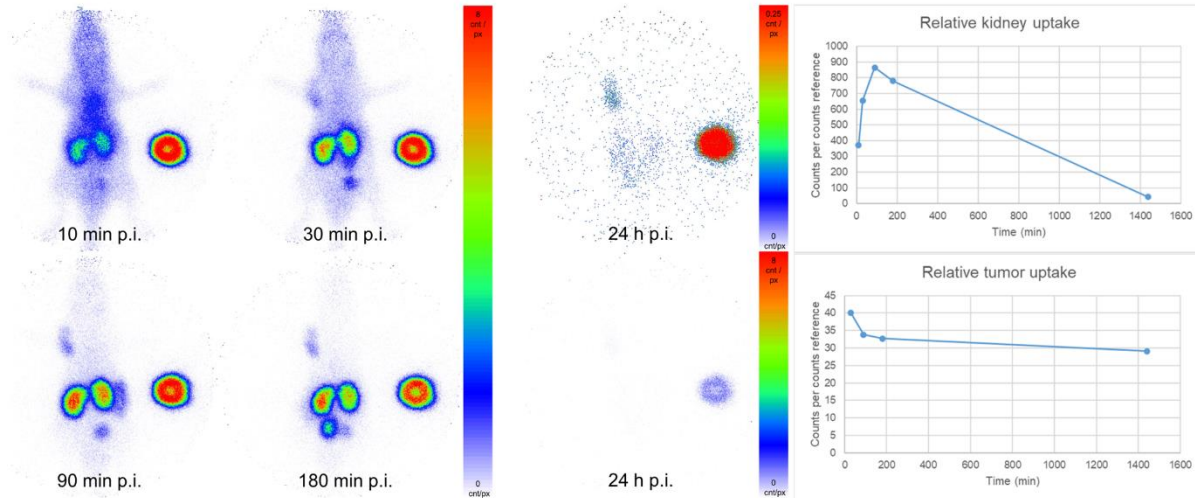
390



391

392 *Figure 2: Dual-photo-peak imaging for intra-individual comparison of Re-PSMA-GCK01 versus Lu-*
 393 *PSMA617 PK*

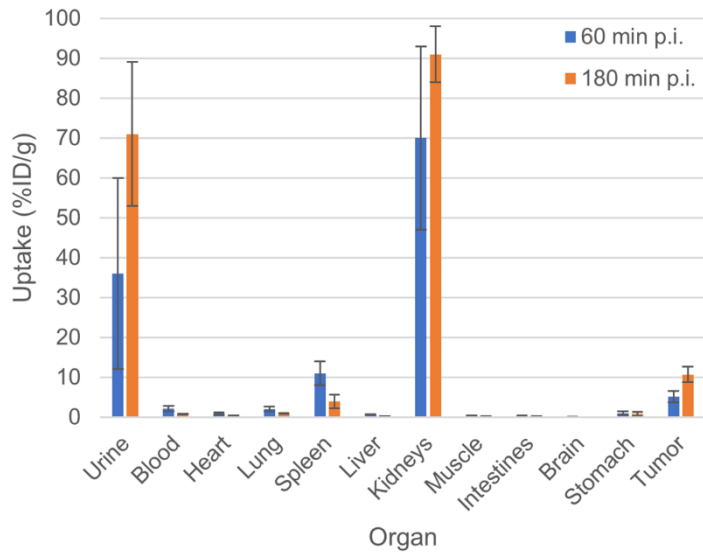
394



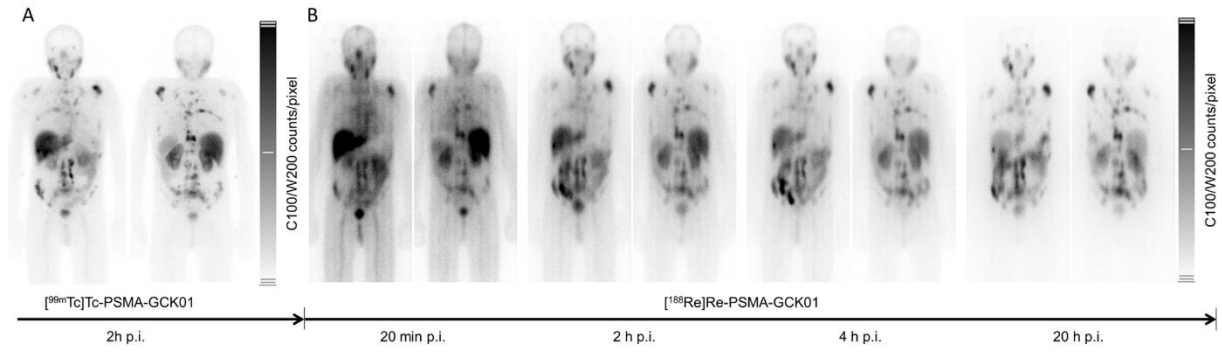
395

396 *Figure 3: Planar imaging of ^{99m}Tc -PSMA-GCK01 in a LNCaP tumor bearing mouse (Red spot at the right*
 397 *side is an internal standard).*

398



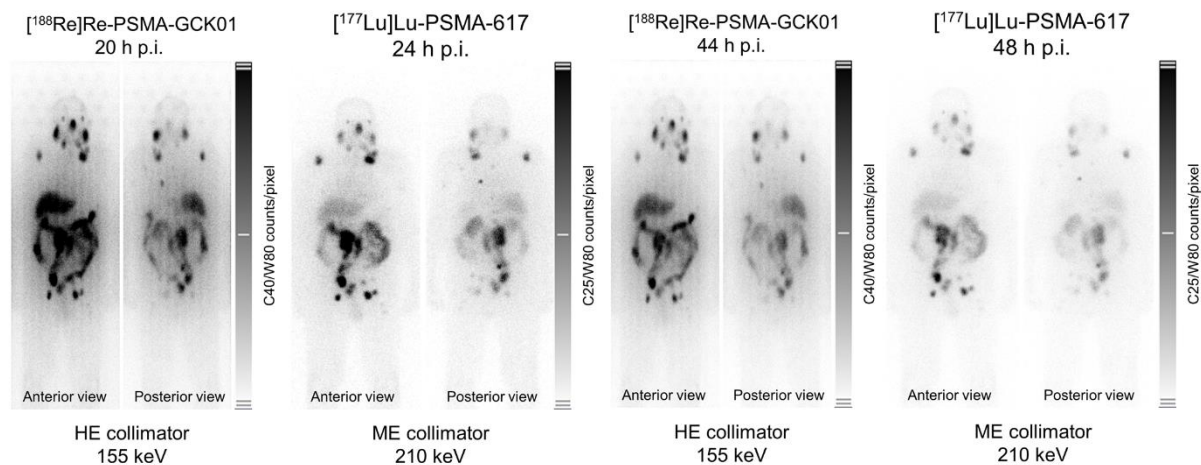
399
 400 *Figure 4: organ distribution of approx. 1 MBq ¹⁸⁸Re-PSMA-GCK01 in LNCaP tumor bearing mice (n = 3 per*
 401 *timepoint). Exact values are provided in supplementary Table 1.*
 402



403

404 *Figure 5: $^{188}\text{Re-GCK01}$ PK (sequential imaging)*

405



406
 407 *Figure 6: Intra-individual comparison of 3.7 GBq Lu-PSMA-617 and 3.7 GBq Re-PSMA-GCK01 at 20-24 and*
 408 *44-48h p.i., respectively.*

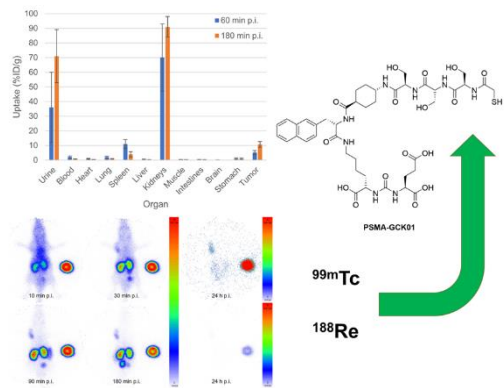
409

410 *Table 1: Binding characteristics of ^{99m}Tc-EDDA/HYNIC-iPSMA and ^{99m}Tc-PSMA-GCK01*

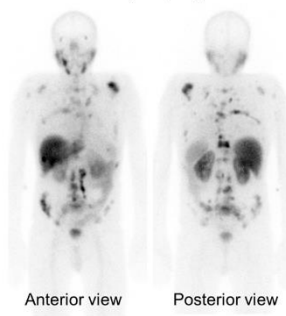
Substance	Uptake [%AD/10 ⁶ cells]	Unspecific uptake [%AD/10 ⁶ cells]	Specific uptake [%AD/10 ⁶ cells]	Ki [nm]
^{99m} Tc-EDDA/HYNIC-iPSMA (reference compound)	20.3±0.3	1.64±0.07	18.7±0.3	38
^{99m} Tc-PSMA-GCK01	19.6±4.8	1.2±0.6	18.4±4.2	26

411

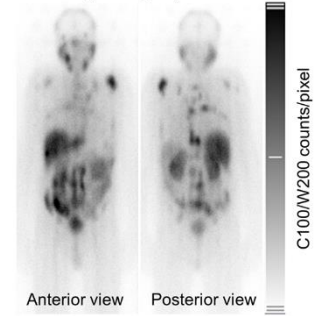
412



^{99m}Tc -PSMA-GCK01
(2h p.i.)



^{188}Re -PSMA-GCK01
(20 h p.i.)



413

414 Graphical Abstract

PSMA-GCK01 - A Generator-Based ^{99m}Tc -/ ^{188}Re -

Theranostic Ligand for the Prostate-Specific Membrane

Antigen

Supplementary information

Contents

S1: Preparative Methods & Cell Culture	1
<i>Preparation of the Precursor</i>	1
<i>Preparation of [^{99m}Tc]Tc-PSMA-GCK01 for in vitro analysis</i>	1
<i>Cellular uptake and competitive binding</i>	2
<i>Plasma protein binding and stability</i>	2
<i>Toxicological investigation of PSMA-GCK01</i>	3
S2: Analytical Methods	3
a) <i>Identity of the precursor (HPLC-MS)</i>	3
b) <i>Purity of the precursor</i>	4
c) <i>Radiochemical purity</i>	5
d) <i>Purity of the [^{99m}Tc]Tc-PSMA-GCK01 formulation</i>	5
e) <i>Purity of the [^{188}Re]Re-PSMA-GCK01 formulation</i>	6
f) <i>Plasma Stability of [^{99m}Tc]Tc-PSMA-GCK01</i>	8
S3: Detailed results of the organ distribution experiment	9

24 **S1: Preparative Methods & Cell Culture**

25 *Preparation of the Precursor*

26 The synthesis of the pharmacophore was accomplished by a well-known procedure: The isocyanate of the
27 glutamyl moiety was generated *in situ* by adding a mixture of 3 mmol of bis(tert-butyl) L-glutamate
28 hydrochloride and 1.5 mL of N-ethyl-diisopropylamine (DIPEA) in 200 mL of dry CH₂Cl₂ to a solution of 1
29 mmol triphosgene in 10 mL of dry CH₂Cl₂ at 0°C over 4 h. After agitation of the reaction mixture for 1 h at
30 25°C, 0.5 mmol of the resin-immobilized (2-chloro-tritylresin) ε-allyloxycarbonyl protected lysine in 4 mL
31 DCM was added and reacted for 16 h with gentle agitation. Subsequently the resin was filtered off and
32 dried.

33 For the synthesis of the precursor, an aliquot of the resin carrying approx. 50 μmol pharmacophore was
34 used. For deprotection, the resin was swollen in CH₂Cl₂ (Dichloromethane, DCM) and reacted with a
35 mixture of 10 mg (PPh₃)₄Pd⁰ and 60 mg dimethylaminoborane in 3 mL DCM for 15-30 minutes.
36 Subsequently the resin was washed with DCM, 5% aminoethanol in DCM (5 min shaking), Methanol,
37 Dimethylformamide (DMF) (3-5 times each).

38 The linker was build-up by means of standard solid phase peptide synthesis (SPPS) using
39 fluorenylmethoxycarbonyl (Fmoc) as protective group. Each coupling was conducted with 3 equivalents of
40 the respective Fmoc protected amino acid, 2.96 equivalents of HATU and 8-12 equivalents of
41 diisopropylamine (DIPEA) for 30 minutes at room temperature under agitation in DMF. Removal of the
42 fmoc group was conducted by reaction with 20 % piperidine in DMF for 5 minutes at room temperature (3
43 times each). Between the individual steps, the resin was washed with DMF (5 times each).

44 The chelator consists of 3 D-Serines (tert-Butyl protected OH) and a terminal mercaptoacetyl group and was
45 build using the same procedure as described for the linker. The coupling of the mercaptoacetyl group was
46 conducted using acetyl protected 2-mercaptoacetic acid (same procedure as for the linker/chelator). For
47 removal of the terminal acetyl-protective group, the solvent was changed to acetonitrile (MeCN) and the
48 deprotection was conducted with 35 μl hydrazinehydrate in 2 mL MeCN for 10-20 minutes at room
49 temperature under agitation. Then the resin was washed with MeCN, DMF and DCM (5 times each). Finally,
50 the compounds were cleaved from the resin using TFA containing 2.5 % water and 2.5 % triisopropylsilane
51 (TIS) (2-3 mL) for 30-45 min at room temperature. The cleavage cocktail was filtered, diluted with 20 mL
52 DCM and the solvents removed under reduced pressure. The crude product was purified by preparative
53 HPLC. Identity of the compounds was confirmed by HPLC-MS (Figure S1) and the purity observed by HPLC
54 (Figure S2).

55

56 *Preparation of [^{99m}Tc]Tc-PSMA-GCK01 for in vitro analysis*

57 Phosphate buffer was prepared from 890 mg Na₂PO₄·2 H₂O in 9.5 mL water for injection and 0.5 mL 2 M
58 NaOH. After dissolution of the salts, the buffer was sterile filtered, the pH was determined using pH stripes
59 (pH = 11.5-12.0). The labeling mixture consisted of 1 μl precursor solution (1 mg / mL in MeCH₂/H₂O 20:50;
60 approx. 1 nmol), 20 μl phosphate buffer, 10 μl tris-carboxyphenylphosphin (TCEP; 28.7 mg / mL in
61 phosphate buffer; 0.1 molar solution) and 4-10 μl pertechnetate in saline (0.9 % NaCl; generator eluate)
62 containing an activity of approx. 7.5 MBq. The mixture was filled to 100 μl with saline (0.9 % NaCl; 59-65

63 μL). The pH of the reaction mixture was 8.0-8.5 (tendency towards 8.5). The mixture was heated at 98 °C
64 for 10 minutes. After cooling to room temperature, the mixture was diluted to 1 mL by addition of saline
65 (0.9 % NaCl, ligand concentration approx. 1 μM). An aliquot was analyzed by HPLC to determine the
66 radiochemical yield (RCY) (Figure S4). Aliquots of the product mixture containing the $^{99\text{m}}\text{Tc}$ -labeled ligand
67 were further diluted to a concentration of approx. 100 nM (precursor) in PBS with and without a 10000
68 fold excess of 2-(Phosphonomethyl)-pentandioic acid, 2-Phosphonomethyl pentanedioic acid (2-PMPA) as
69 competitor.

70

71 *Cellular uptake and competitive binding*

72 LNCaP (lymph node carcinoma of the prostate; CRL-1740; DSMZ-German Collection of Microorganisms
73 and Cell Cultures GmbH, Braunschweig, Germany) cells were seeded in 6-Well plates in RPMI medium
74 containing 20 % FBS (Pan Biotech, Aidenbach, Germany) and grown to a confluency of 70-80 % in an
75 incubator at 37°C with humidified air equilibrated with 5% CO₂ (approx. 2 days).

76 Prior to the uptake experiment, the medium was removed and the cells were incubated with 1 mL of a 1
77 nM ligand solution prepared by 1:99 dilution in RPMI medium of the 100 nM ligand formulations with and
78 without competitor for *in vitro* analysis (see supporting information). After 1 h the medium containing the
79 $^{99\text{m}}\text{Tc}$ -ligand was removed, the cells were washed twice with 1 mL PBS and lysed twice using lysis buffer
80 (0.3 M NaOH containing 0.2 % SDS; 700 μL each). The cellular uptake was determined from the activity in
81 the lysed fraction. The unspecific uptake was determined from the cellular uptake of the cells incubated
82 with the ligand in presence of the competitor. Each experiment was conducted as triplicate.

83 For determination of K_i, competitive binding experiments were conducted. Four six-well plates were
84 prepared as described above. After removal of the medium the cells were incubated with 1 mL of a 1 nM
85 ligand solution prepared by 1:99 dilution of the 100 nM ligand formulations for *in vitro* analysis (without
86 competitor; see supporting information) in RPMI medium containing different concentrations of
87 competitor (2-PMPA, 10E-4/-5/-6/-7/-8/-9 mol/L). Further processing was conducted as described above.

88 *Plasma protein binding and stability*

89 Blood was drawn from 3 volunteers and the plasma was separated by centrifugation at 2000 RPM. 400 μL
90 Plasma were incubated at 37 °C with 100 μL $^{99\text{m}}\text{Tc}$ -PSMA-GCK01 (clinical protocol / approx. 150 MBq/mL).

91 For Plasma protein binding, 100 μL of the test solution were removed after 1 h of incubation, diluted with
92 0.9 % saline and an ultra-filtration was performed with 500 μL of the dilution using Amicon Ultracel 3k
93 centrifugal filters (Merck Millipore Ltd, Corck, Ireland) in an Eppendorf Centrifuge was performed at 12k
94 RPM. The filter was subsequently washed with 400 μL saline and the unified filtrates, as well as the filter
95 unit were measured on a Gamma counter.

96 For plasma stability, 400 μL MeCN were added to 100 μL test solution for protein precipitation (after 1, 2
97 and 4 h of incubation). The mixture was centrifuged at 13k RPM for 5 minutes and 100 μL of the solution
98 were pipetted into another Eppendorf vessel. The protein precipitation was completed by addition of
99 another 100 μL MeCN and subsequent centrifugation at 13k RPM for 5 minutes. Then, the plasma free
100 fraction was analyzed using Gamma-HPLC.

101 **Toxicological investigation of PSMA-GCK01**
 102 A toxicological investigation of PSMA-GCK01 was conducted under full GLP by an external facility (Agilex
 103 Biolabs, Thebarton, Australia) under study number TLX-003. Briefly, animals (Healthy CD-2 mice, 6-8
 104 Weeks old, 30-40 g) were divided into three groups and received daily repetitive dose 0.0 mg/kg (vehicle),
 105 0.2 mg/kg (low dose) and, 2.0 mg/kg (high dose) PSMA-GCK01. The animals were either sacrificed one day
 106 (Main) or 14 days (Recovery) after receiving the final dose of PSMA-GCK01 and investigated by adequate
 107 pathological procedures. The design of this study was adapted from and is in accordance with OECD
 108 guideline for testing of chemicals (No. 407).

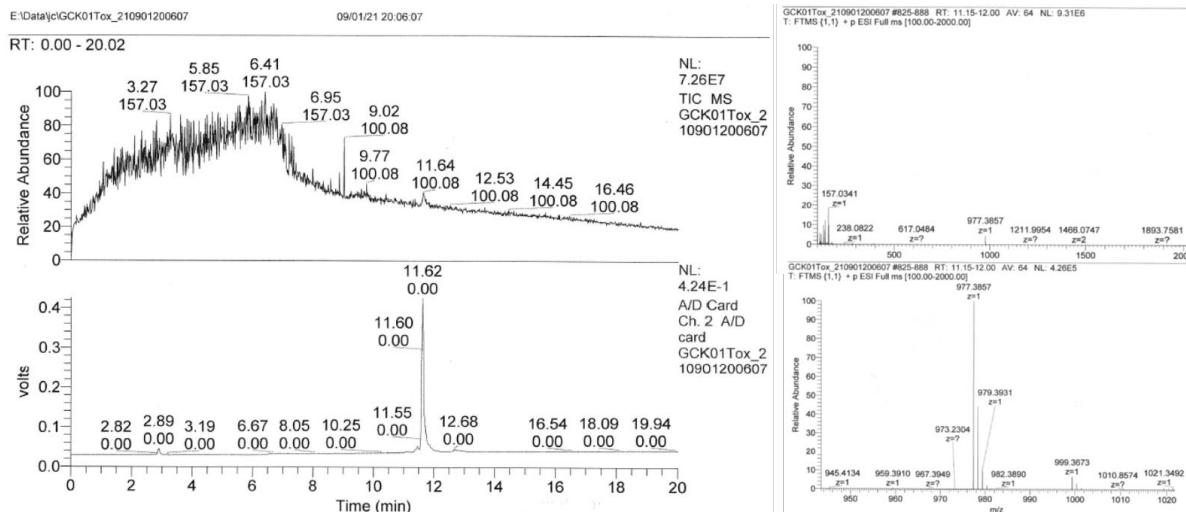
109

110 S2: Analytical Methods

111 a) Identity of the precursor (HPLC-MS)

112 HPLC-MS (gradient A: 0 % A (0min) 100 % A (20 min) linear gradient, 0.2 mL/min; A + B = 100 %;
 113 solvent A: MeCN + 0.1 % trifluoroacetic acid, solvent B: water + 0.1 % trifluoroacetic acid; Column:
 114 Hypersil Gold aQ 200X2.1 mm, 1.9 μ m particle size).

115 Analysis was conducted on an Agilent Infinity 1200 System with binary pump (Bin Pump SL),
 116 autosampler (HIP ALS SC), column compartment (Col Comp), and an UV detector (VWD SC+). The
 117 system was connected to a Thermo Fisher Exactive ESI MS system. The system was controlled by
 118 Thermo Xcalibur Version 3.0.63. Confirmation of identity is assessed by comparing the
 119 mass/charge values in the resulting integrated electropherograms (Figure S1).
 120

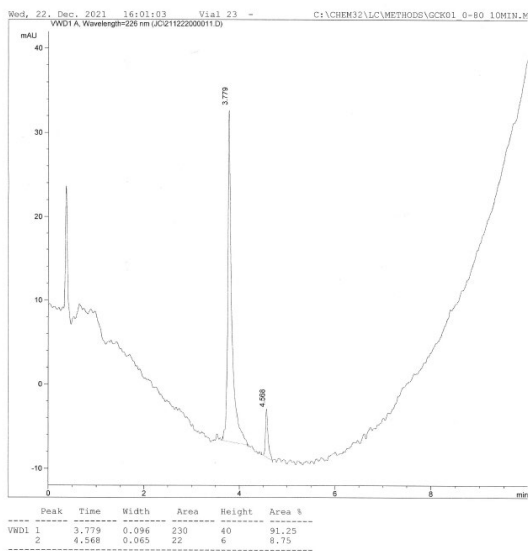


121
 122 **Figure S1: HPLC-MS after separation of PSMA-GCK01 precursor; Identity is confirmed by the peak at $m/z = 977.386$ (calc. m/z**
 123 **$([M+H]^+) = 977.392$) and $m/z = 999.367$ (calc. m/z $([M+Na]^+) = 999.374$)**

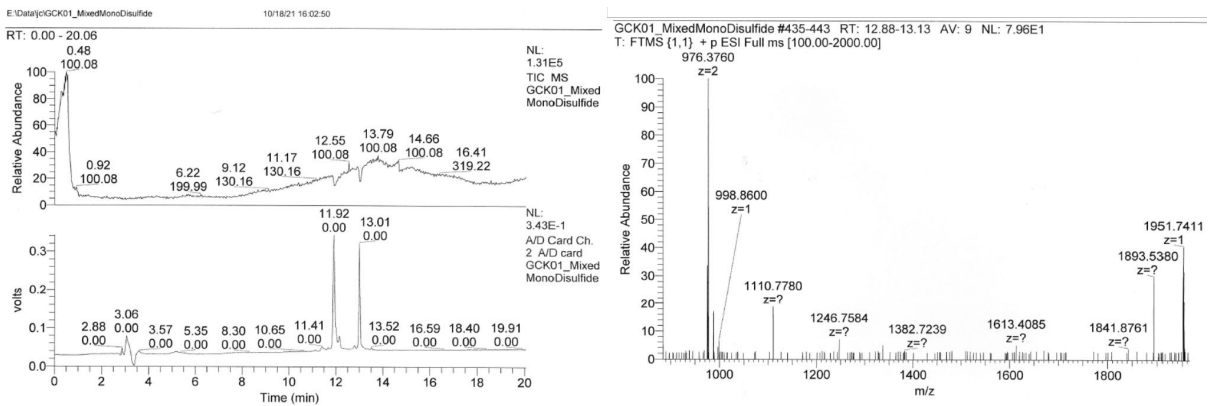
124

125 **b) Purity of the precursor**
 126 HPLC-gradient: 0 % A (0min) 80 % A (10 min) linear gradient, 2 mL/min; A + B = 100 %; solvent A:
 127 MeCN + 0.1 % trifluoroacetic acid, solvent B: water + 0.1 % trifluoroacetic acid; Column:
 128 Chromolith Performance C18e 100X3 mm). UV detection was carried out at 226 nm wavelength.
 129 Analysis was conducted on an Agilent Infinity 1100 System with binary pump (G1312A Bin Pump),
 130 an autosampler (G1313A ALS), and an UV detector (G1314A VWD). The system was controlled
 131 using ChemStation for LC systems Rev. D.01.03.

132 On the system described above the retention time of PSMA-GCK01 is 3.8 ± 0.2 min and the retention
 133 time of the corresponding disulfide 4.6 ± 0.2 min. A sample chromatogram with visible amounts of
 134 the disulfide is shown in Figure S2. Identification of the disulfide was conducted after intentional
 135 disulfide formation by HPLC-MS (Figure S3).
 136



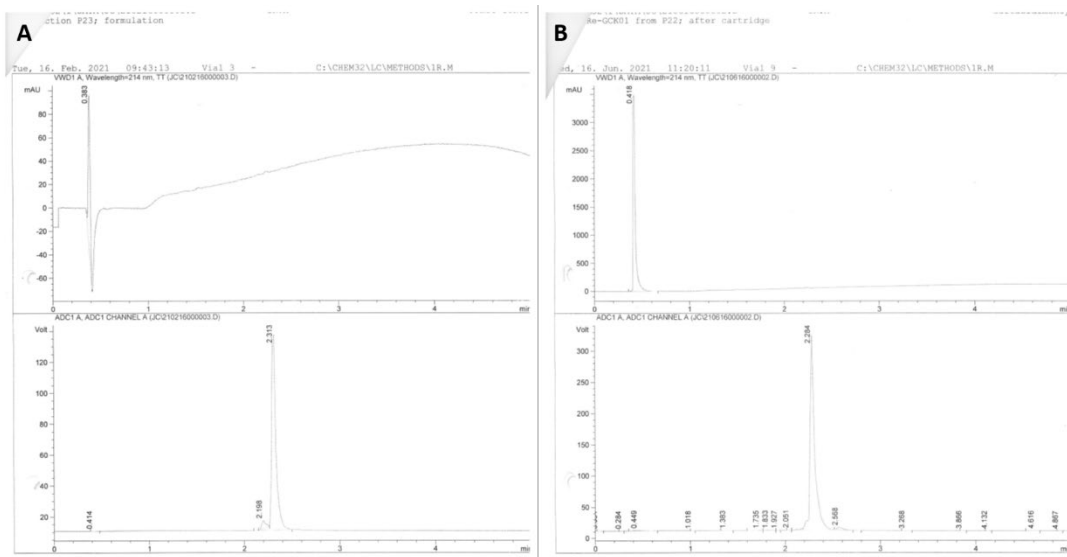
137
 138 **Figure S2: HPL-Chromatogram of PSMA-GCK01 in solution after some time for oxidation (disulfide formation); Identity of the**
 139 **disulfide was confirmed bx HPLC-MS**



140
 141 **Figure S3: HPLC-MS after separation of PSMA-GCK01 precursor and intentional oxidation period (disulfide formation): Peak at**
 142 **13.01 is the disulfide – The identity is confirmed by the peak at $m/z = 1951.741$ (calc. m/z $[(M+H^+)]^+ = 1951.761$) and $m/z =$**
 143 **976.376 (calc. m/z $[(M+2H^+)]^{2+} = 976.384$.**

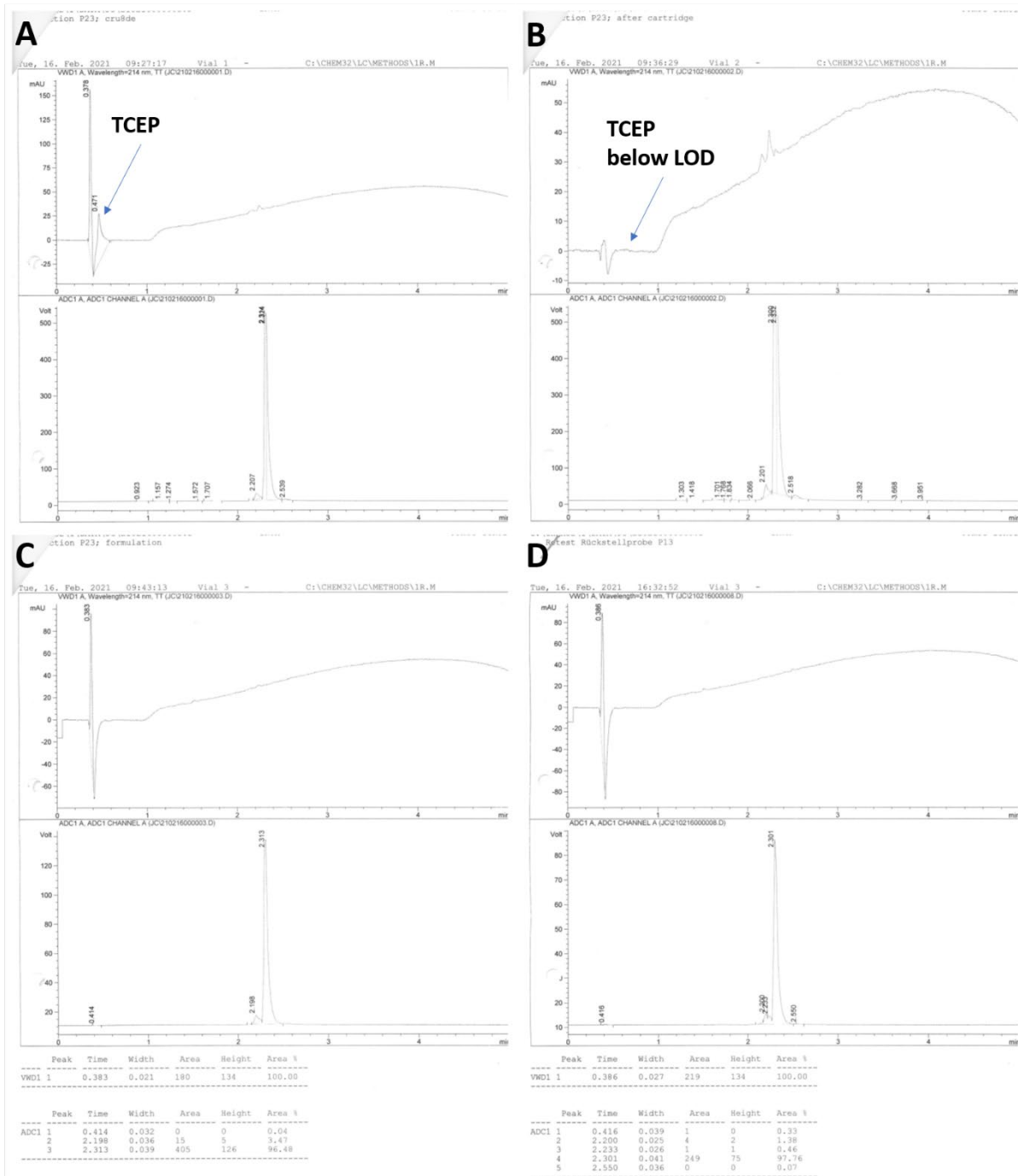
145 **c) Radiochemical purity**
146 HPLC-gradient: 0 % A (0min) 80 % A (5 min) linear gradient, 2 mL/min; A + B = 100 %; solvent A:
147 MeCN + 0.1 % trifluoroacetic acid, solvent B: water + 0.1 % trifluoroacetic acid; Column:
148 Chromolith Performance C18e 100X3 mm). UV detection was carried out at 226 nm wavelength.
149 Analysis was conducted on an Agilent Infinity 1100 System with binary pump (G1312A Bin Pump),
150 an autosampler (G1313A ALS), an UV detector (G1314A VWD) and a gamma-probe (Raytest,
151 Straubenhardt, Germany). The system was controlled using ChemStation for LC systems Rev.
152 D.01.03.

153 On the system described above the retention time of PSMA-GCK01 is 2.30 min, [^{99m}Tc]Tc-PSMA-
154 GCK01 is 2.33 min and the Retention times of [¹⁸⁸Re]Re-PSMA-GCK01 are 2.12 min (undesired
155 isomer) und 2.17 min. Sample chromatograms are shown in Figure S4.
156



157
158 *Figure S4: Typical radiochromatograms of (A) [^{99m}Tc]Tc-PSMA-GCK01 and (B) [¹⁸⁸Re]Re-PSMA-GCK01 (after formulation, each).*

159
160 **d) Purity of the [^{99m}Tc]Tc-PSMA-GCK01 formulation**
161 Several radiochromatograms of [^{99m}Tc]Tc-PSMA-GCK01 are shown in Figure S5: First, in (A) the
162 chromatogram directly after the conjugation reaction is shown. The presence of TCEP is causing a
163 pronounced peak at a retention time of 0.47 minutes (UV-trace). After cartridge separation (B)
164 (before PBS dilution, which would reduce sensitivity by a factor of 10) the TCEP peak is below LOD,
165 demonstration quantitative separation by the cartridge purification process.
166 Second, example chromatograms for the shelf-life are shown in the lower part of Figure S5: In
167 comparison to the formulation at 0h shelf-life (C), no signs of degradation were observed after
168 approx. 7 h at room temperature (D) indicating more than 6 h shelf-life.



169

170 Figure S5: Radiochromatograms from $[^{99m}\text{Tc}]\text{Tc-PSMA-GCK01}$ before (A) and after (B) cartridge separation, formulation (C) and
 171 formulation after 7 h at room temperature (D).

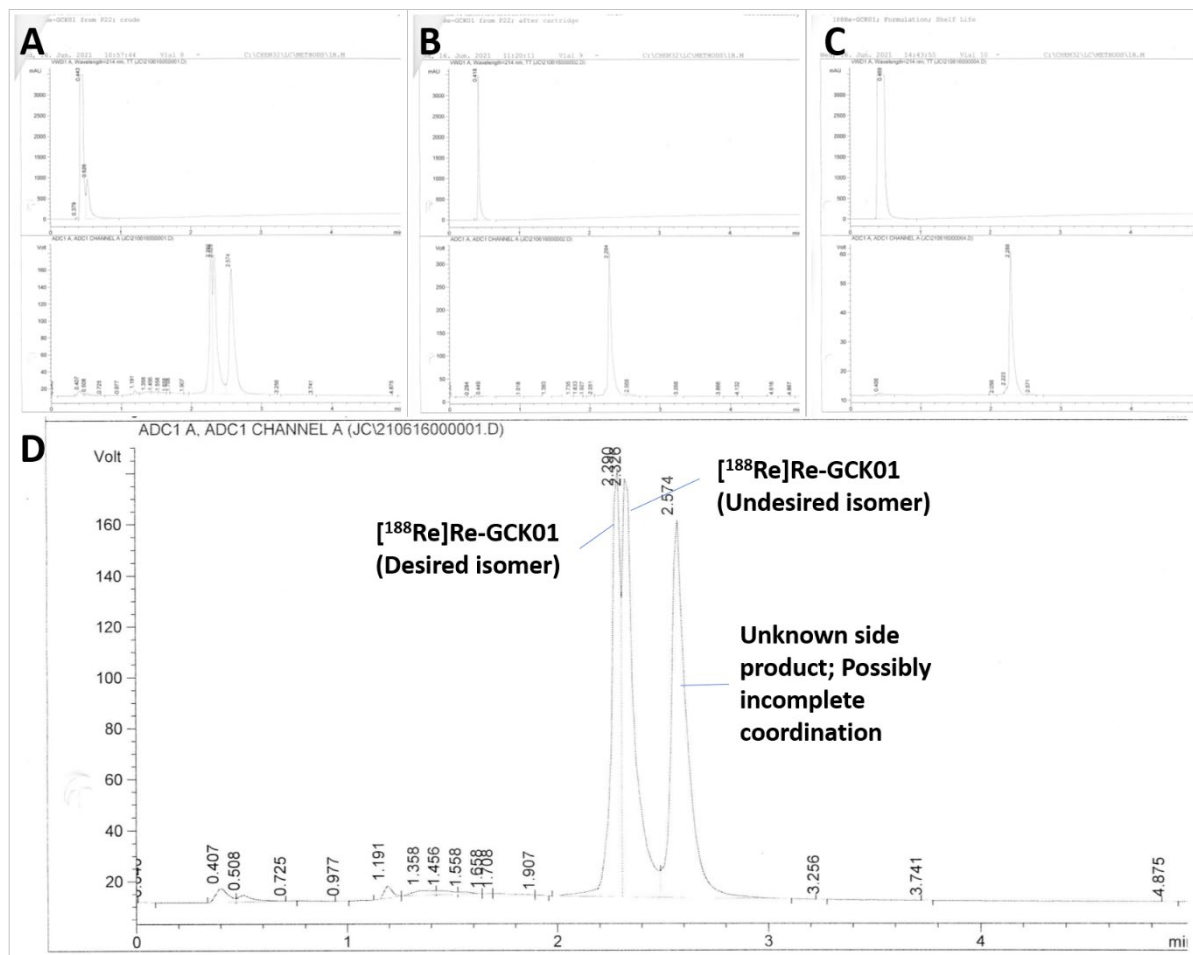
172

173 e) Purity of the $[^{188}\text{Re}]\text{Re-PSMA-GCK01}$ formulation

174 The ^{188}Re -labeling of MAS₃ derivatives (including PSMA-GCK01) does lead to a mixture of
 175 diastereomers. This is shown in Figure S6 A and D. The product at 2.57 min is most likely an
 176 incompletely coordinated intermediate. However, by heating the mixture at elevated pH values

177 (above 7.0) the tracer can be converted to a single isomer, which was used for evaluation of
178 [¹⁸⁸Re]Re-PSMA-GCK01. Since the RCY of [¹⁸⁸Re]Re-PSMA-GCK01 after this conversion step is
179 higher than the RCP of both diastereomers at 2.92-3.32 min (data not shown), we rationalized that
180 the third peak is incomplete coordination. It should be noted that this product is only partially
181 converted to the desired [¹⁸⁸Re]Re-PSMA-GCK01, while a fraction dissociates to free Rhenium.
182 Therefore, cartridge separation is conducted after the conversion step.

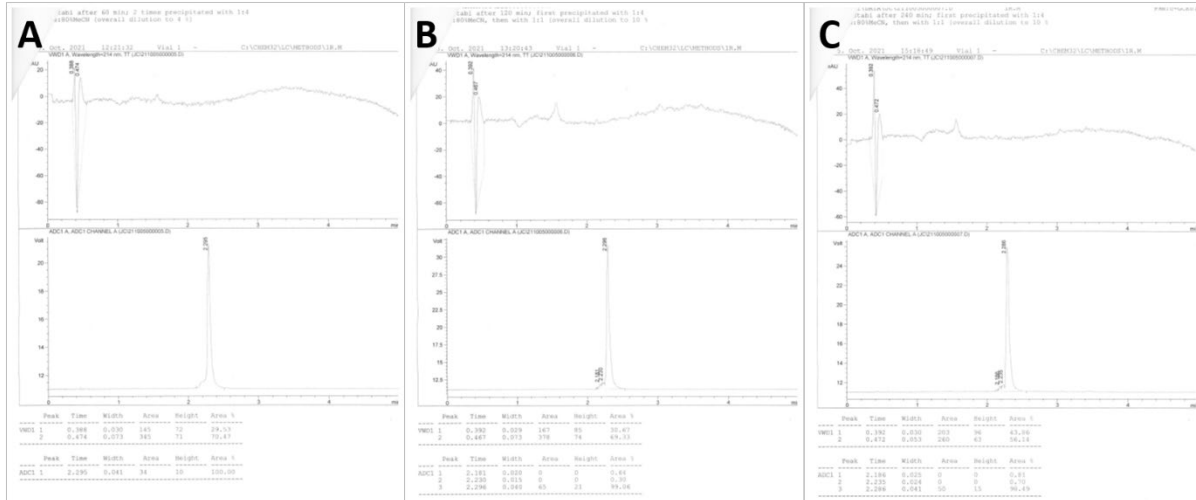
183 An example chromatogram for the shelf-life is shown in Figure S6 (C): Approx. 2.8 % degradation
184 were observed in this case over a period of 3 h at room temperature.



185
186 *Figure S6: Radiochromatograms from [¹⁸⁸Re]Re-PSMA-GCK01 after ¹⁸⁸Re-labeling (A) and after cartridge separation (B),*
187 *formulation after 3 h at room temperature (C) and zoom in chromatogram A (D)*

188
189
190

191 f) Plasma Stability of $[^{99m}\text{Tc}]\text{Tc-PSMA-GCK01}$
 192 Some results from the plasma-stability experiment with $[^{99m}\text{Tc}]\text{Tc-PSMA-GCK01}$ are shown in
 193 Figure S7: No signs of degradation were observed for the plasma free fraction at 60 min (A), 120
 194 min (B) and 240 min (C) incubation time.



195
 196 Figure S7: Radiochromatograms from the plasma stability experiment of $[^{99m}\text{Tc}]\text{Tc-PSMA-GCK01}$
 197
 198

199 **S3: Detailed results of the organ distribution experiment**

200

201 *Table S1: Results of the ex-vivo biodistribution after injection of approx. 1 MBq of the respective [¹⁸⁸Re]Re-PSMA-GCK01*

Organ	%ID/g	%ID/g
	1 h p.i.	3 h p.i.
Urine	36±24	71±18
Blood	2.1±0.7	0.74±0.08
Heart	0.9±0.3	0.46±0.03
Lung	2.0±0.6	1.01±0.08
Spleen	11±3	3.9±1.7
Liver	0.68±0.05	0.28±0.01
Kidneys	70±23	91±7
Muscle	0.3±0.1	0.18±0.06
Intestines	0.36±0.06	0.24±0.04
Brain	0.04±0.02	0.030±0.004
Stomach	1.0±0.5	0.8±0.5
Tumor	5.1±1.4	10.7±1.9

202